

## Combination of GNSS and InSAR for Future Australian Datums

***Thomas Fuhrmann***

Geoscience Australia, Canberra, Australia  
Phone: +61 2 6249 9187, email: thomas.fuhrmann@ga.gov.au

***Matthew Garthwaite***

Geoscience Australia, Canberra, Australia

***Sarah Lawrie***

Geoscience Australia, Canberra, Australia

***Nicholas Brown***

Geoscience Australia, Canberra, Australia

### ABSTRACT

GNSS can provide a temporally dense set of geodetic coordinate observations in three dimensions at a small number of discrete measurement points on the ground. Compare this to the Interferometric Synthetic Aperture Radar (InSAR) technique which gives a spatially dense set of geodetic observations of ground surface movement in the viewing geometry of the satellite platform, but with a temporal sampling limited to the orbital revisit of the satellite. Using both of these methods together can leverage the advantages of each to derive more accurate, validated surface displacement estimates with both high temporal and spatial resolution. In this paper, the properties of both techniques are discussed with a view to combined usage for future Australian datums. Differential GNSS processing is applied to data observed at a local geodetic network in the Sydney region as well as time series InSAR analysis of Radarsat-2 data. Surface displacements resulting from the two techniques are compared and validated at 21 geodetic monitoring sites equipped with GNSS and radar corner reflectors (CRs). The resulting GNSS/InSAR displacement time series agree at the level of 5 to 10 mm. This case study shows that the co-located GNSS/CR sites are well-suited to compare and combine GNSS and InSAR measurements. An investigation of potential multipath effects introduced by the CRs attached directly to GNSS monumentation found that daily site coordinates are affected at a level below 0.1 mm. The GNSS/CR sites may hence serve as a local tie for future incorporation of InSAR into national datums.

**KEYWORDS:** GNSS, GPS, InSAR, Combination, Datums, Surface Displacements, Geodetic Networks

## 1. INTRODUCTION

With the establishment of the Geocentric Datum of Australia 2020 (GDA2020) in October 2017, Australia has aligned its national coordinate reference frame more closely to satellite navigation constellations (Warrington 2017). Plate tectonic movements generate a need to frequently update coordinates of fixed benchmarks since otherwise static horizontal coordinates would differ from GNSS measurements at the metre level within 15 years (where the rate of movement of the Australian plate is 7 cm per year, see ICSM 2017). However, the current datum considers the general movement trend of the Australian plate only and does not account for local deformation of the Earth's surface. Local deformation may occur for various reasons and induce coordinate changes of an even greater magnitude. The source of deformation can be natural (e.g. intra-plate tectonics, landslides or groundwater changes) or anthropogenic (e.g. subsurface mining or construction activities). Continental plate tectonics mainly involve horizontal surface movements, whereas local deformation may cause significant vertical movements that will affect the vertical datum.

Currently, the only way to update benchmark coordinates affected by surface deformation is to remeasure the coordinates by conducting a repeat GNSS or levelling survey, which is time-consuming and expensive. Within this paper, the use of satellite radar remote sensing is proposed to characterise local surface deformation, and to update coordinates and datums on a routine basis. Interferometric Synthetic Aperture Radar (InSAR) is an active satellite remote sensing technique which enables the detection of millimetre to centimetre level movements of the Earth's surface (Casu et al., 2006; Ferretti et al., 2007). In contrast to the point-wise information provided by GNSS or levelling, InSAR can cover large areas at high spatial resolution and is hence well-suited to cover the full spatial extent of most surface deformation phenomena. High accuracy for the horizontal coordinate and displacement components is obtained from GNSS, whereas InSAR is more sensitive to detecting vertical surface displacements. Therefore, combining the two techniques makes use of their complementary properties regarding spatial and temporal resolution as well as sensitivity to different displacement components.

The major objective of the work presented here is to investigate the potential for improving the spatial and temporal resolution of geodetic datums in Australia by routinely combining these independent geodetic data in the future. For this purpose, data from a local geodetic network is analysed since July 2016 comprising of 21 geodetic monitoring sites in the Sydney region. The geodetic network covers an area of about 20 km x 20 km. Each site consists of a co-located GNSS antenna and two corner reflectors (CRs), which reflect the radar signal back to the sensor with a high signal-to-noise ratio and are exploited in the InSAR analysis. These geodetic monitoring sites serve as a proof of concept that InSAR measures the same deformation signal as observed by GNSS and, in addition, provides the opportunity to conduct a local tie between the techniques.

## 2. GEODETIC METHODS

This section gives a brief overview on how surface displacements are derived from GNSS and InSAR data as well as on the major characteristics of both geodetic techniques. Furthermore some remarks on radar CRs and local ties between GNSS and InSAR at co-located sites are given.

## 2.1 Surface Displacements from GNSS

As a first analysis step, 3D position coordinates are estimated from GNSS observations during a certain time period (e.g. one daily coordinate estimate from 24 hours of GNSS observations). Surface displacements are subsequently derived as a change of position over time. A relative (or differential) positioning strategy enables most of the perturbation terms affecting GNSS signals to be eliminated or at least reduced by combining observations of different satellites and receivers at different measurement epochs (e.g. Hofmann-Wellenhof et al., 2008). Differential GNSS analysis makes use of a network of surrounding reference sites and is suitable to estimate coordinates of a local network at high precision (e.g. Torge and Müller, 2012).

The GNSS data presented in Section 3 is analysed as a differential network using a stochastic connection to surrounding IGS sites (i.e. seven sites located on the Australian tectonic plate) and surrounding APREF sites (Asia Pacific Reference Frame; i.e. ten sites at distances between 30 and 700 km from the area of interest). The results are daily site coordinates (XYZ) in ITRF2014 (Altamimi et al., 2016). The major displacement trend follows the movement vector of the Australian tectonic plate at the site position. In order to obtain local deformation, the linear trend is calculated at each GNSS site from an Australian tectonic plate model (see ICSM 2017) and subtracted from the XYZ time series. Subsequently, XYZ coordinates are transformed to longitude, latitude and ellipsoidal height. The first daily coordinate estimate serves as a temporal reference and is set to zero. Finally the longitude, latitude and height differences with respect to the first day are transformed to topocentric metric coordinate differences (East, North, Up) using the local radii of curvature of the Ellipsoid. Table 1 summarises the characteristics of surface displacements derived from GNSS using the described method. Note that precision of the Up component is a factor of three poorer than the horizontal components. This is because visible GNSS satellites are only distributed in the hemisphere above the local horizon (e.g. Choi et al., 2007).

	<b>Temporal resolution</b>	<b>Spatial resolution</b>	<b>Spatial reference</b>	<b>Precision</b>	<b>Sensitivity to East, North, Up</b>
<b>GNSS:</b>	high: daily (for continuously operating sites)	low: point-wise, at least several km between points	reference sites used for diff. processing	high: 1 mm horizontal, 3 mm vertical	high, high, medium
<b>InSAR:</b>	medium: weeks to months (24 days)	high: pixel size of the sensor (9 m x 9 m pixels)	single chosen reference area	medium: 3-6 mm (for C-Band sensors)	medium, low, high

**Table 1.** Characteristics of GNSS and InSAR with respect to surface displacement estimation, values given in brackets for spatial and temporal resolution of InSAR relate to the Radarsat-2 data used within this paper

## 2.2 Surface Displacements from InSAR

Spaceborne synthetic aperture radar (SAR) systems measure the range (i.e. the distance to the detected object) and the intensity of radar backscattering from the ground surface. From their side-looking image geometry, SAR sensors provide a 2D map of the Earth's surface in the coordinate system of the platform. As for GNSS, the distance to an object is expressed by a phase measurement. InSAR is a processing technique that makes use of two or more SAR images acquired at different times to derive relative surface displacements from changes in

the measured phase signal. When a stack of SAR data is available, images of phase difference are calculated (so-called “interferograms”) resulting in a displacement time series for each pixel in the aligned images. However, the phase information may be noisy at some pixels if the backscattering characteristics of the ground changes through time, particularly in vegetated areas. Ferretti et al. (2000, 2001) introduced the concept of Persistent Scatterers (PS) which makes use of a subset of pixels with consistent backscattering through time. At these PS pixels, the phase signal is analysed and other nuisance terms contributing to the signal, such as atmospheric or orbital effects, are separated from the phase related to surface displacement (e.g. Hooper et al., 2004; Hooper et al. 2007; Adam et al., 2003; Kampes, 2005). The remaining phase is subsequently transformed to a metric displacement using the wavelength of the radar sensor. Common radar wavelengths used by SAR satellite sensors are 3.1 cm (X-band), 5.6 cm (C-band) and 23.6 cm (L-band).

As for GNSS displacement analysis, a spatial and temporal reference has to be defined during the processing. In the case of InSAR, the spatial reference must be located within the imaged area. It is common practice to choose an area presumed to be stable and containing several hundreds to thousands of PS pixels. All displacements can then be interpreted relative to this presumably stable reference area. The temporal reference is restricted to the SAR image acquisition dates, e.g. the first acquisition of a given image stack can be used as a temporal reference. Table 1 summarises the characteristics of surface displacements derived from InSAR. Note that displacements from InSAR are derived along a slanted, 1D line of sight (LOS) towards the satellite. As radar satellites are acquiring image data of the same area on ascending (travelling south to north) as well as descending (travelling north to south) orbital passes, LOS displacements can be mathematically transformed to East-West and Up-Down components when information from both orbital viewing geometries is present at the same location and over the same period of time. Sensitivity to North-South displacements is low due to the polar orbit of all SAR satellites and the side-looking image geometry.

### **2.3 Co-located GNSS/InSAR sites using Radar Corner Reflectors**

Generally, the exact position of radar backscattering within a PS pixel is unknown. However, artificial targets designed to backscatter a high proportion of incident radar energy, such as radar corner reflectors (CRs), enable the absolute position of a PS pixel to be known. CRs can therefore be used to validate and combine InSAR with other geodetic techniques for surface displacement analysis. Furthermore, geodetic monitoring sites consisting of a GNSS antenna and a CR may serve as a local tie to connect InSAR observations into future Australian Datums. The national network of GNSS sites provides a large-scale absolute reference frame which could be densified using information on local deformation derived from InSAR in the future. In this case the local tie of GNSS and InSAR connects relative displacements derived from InSAR on adjacent satellite tracks to absolute displacements derived by the national GNSS network.

A CR reflects incoming electromagnetic energy transmitted from the satellite to the ground directly back to the receiving antenna of the satellite. The amount of energy received at the SAR sensor depends on the size, shape and material of the reflector as well as on the orientation of the reflector with respect to the transmitted signal. A detailed description on suitable sizes for CRs used with commonly employed SAR frequencies as well as considerations with respect to manufacturing and long-term installation of these artificial targets is given by Garthwaite et al. (2015) and Garthwaite (2017). Figure 1 shows an

example of a co-located geodetic monitoring site consisting of GNSS antenna/receiver and ascending/descending CRs as used for the case study described in Section 3. Note that the CR apex point is offset from the GNSS antenna reference point, meaning that displacements resulting from GNSS and InSAR analyses are not measured at the exact same location. When comparing displacements measured at the GNSS antenna and at ascending and descending CRs, it is implicitly assumed that the CRs will observe the same magnitude and direction of movement as the antenna on top of the pole.

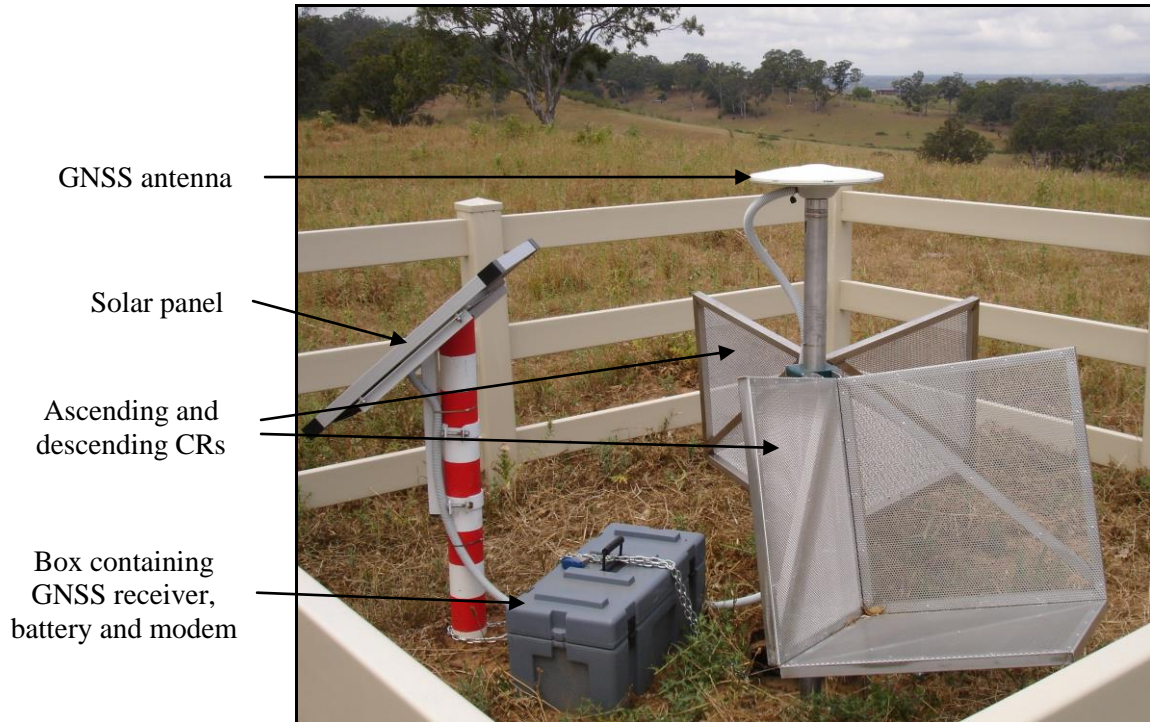


**Figure 1.** Geodetic monitoring site CA19; GNSS observations are acquired continuously at this site, the CRs are oriented for SAR signals transmitted by the Radarsat-2 satellite on ascending and descending orbital passes with a repeat time of 24 days on each pass

### 3. CASE STUDY IN THE SYDNEY REGION

This section presents the case study to combine surface displacements from GNSS and InSAR in the Sydney region, NSW. The case study area and database are described (Section 3.1) as well as the displacement results (Section 3.2). Section 3.3 presents the results of an investigation in to the potential multipath effects that could be introduced by CRs attached directly to GNSS monumentation.

#### 3.1 Case Study Area and Database

The case study area and the available data sets are shown in Figure 2. Radarsat-2 data were acquired on one ascending and one descending track with a 24 day repeat time since July 2015. Figure 2 also displays the GNSS sites located within the area of interest. Three of the sites are part of CORSnet-NSW and operated by NSW Spatial Services (i.e. sites CRDX, PCTN and MENA). In cooperation with NSW Spatial Services, CRs have been attached to the GNSS monument at site MENA in May 2016, see Section 3.3. In addition, 20 new



geodetic monitoring sites were established in May/June 2016 consisting of the setup shown in Figure 1. Most of these new sites are operated on a campaign basis, which means with 24 hours of GNSS observations being acquired at monthly intervals since July 2016. Four of the new sites are operated continuously.

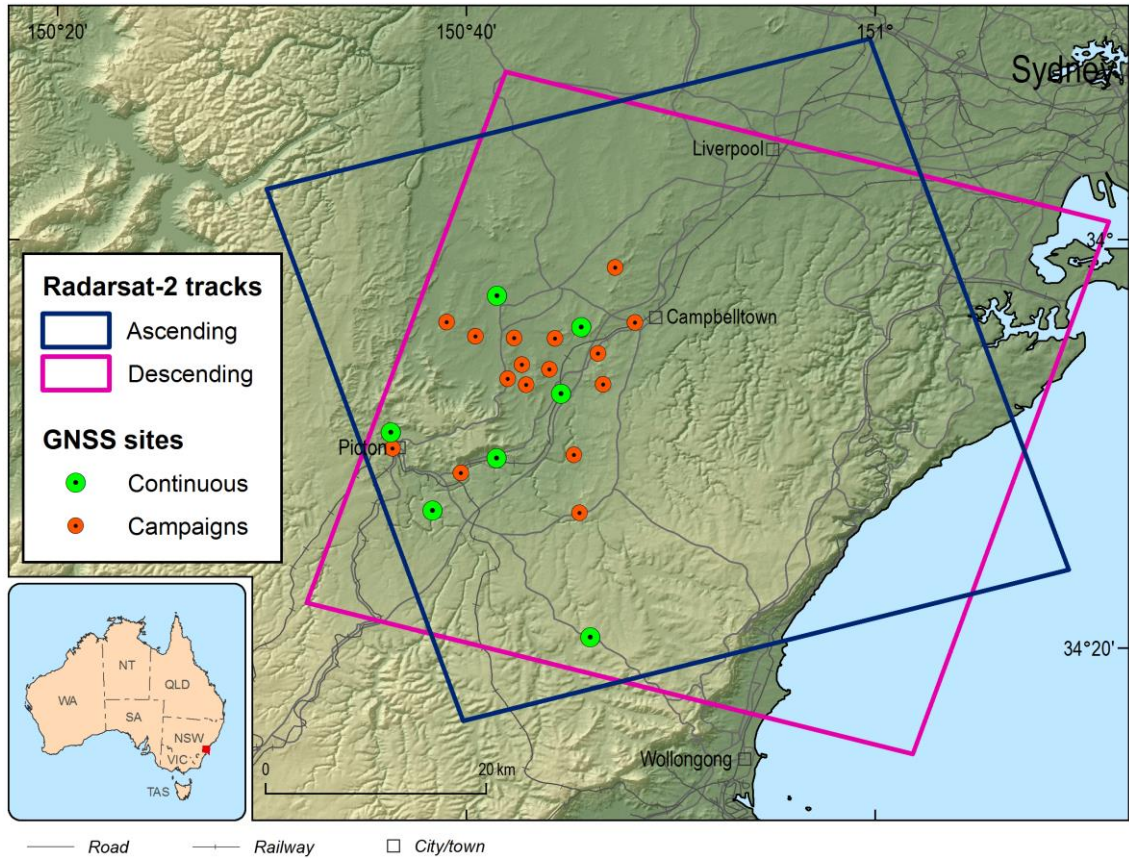


**Figure 2.** Overview of the database: GNSS sites and SAR tracks in ascending and descending geometries; Background: Digital Elevation Model

### 3.2 Results: Surface Displacements

The GNSS database is analysed as described in Section 2.1 using the Bernese GNSS Software (Dach et al. 2015) to calculate XYZ coordinates for each site and each analysed day. Note that for consistency with the surrounding reference network, only GPS data has been analysed to estimate daily site coordinates. Figure 3 displays the resulting coordinate time series at continuously operating site CA19 after subtraction of the general trend of the Australian Plate. This site is affected by strong horizontal motion particularly at the beginning of the time series. The total horizontal displacement sums up to about 5 cm in the Southeasterly direction. The resulting coordinate time series for the Up component is noisier than the East and North components. This is because vertical coordinate estimates and corresponding coordinate changes are less accurate compared to horizontal coordinate estimates. Despite this, a slight downward displacement trend totalling about 1.5 cm can be observed at CA19. Mean coordinate standard deviations ( $2\sigma$ ) are 1.1 mm and 2.9 mm for horizontal and vertical components, respectively.

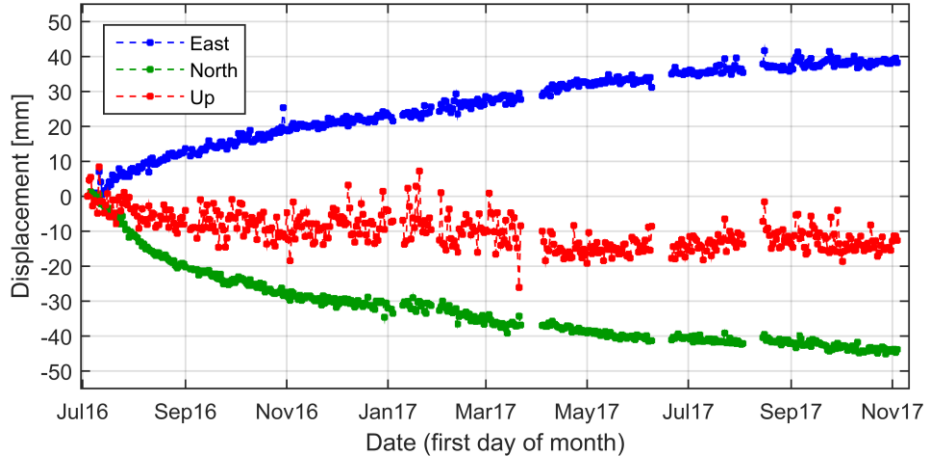


**Figure 3.** Displacement (i.e coordinate changes in East, North and Up component) at site CA19 with respect to the first observed day (4 July 2016)

Although all three dimensions of the displacement vector can be observed from GNSS analysis, only 1D information in the LOS is provided by a single InSAR analysis. However, instead of a point-wise displacement, InSAR is able to provide a spatially dense image of surface displacements. Figure 4 displays linear displacement rates for the area of interest derived from separate PS-InSAR analyses as described in Section 2.2 for the ascending and descending Radarsat-2 tracks between July 2015 and October/November 2017. Note that the displacements are observed along the slanted LOS towards the satellite which is different for the ascending and descending image geometries: the ascending pass observes the ground at an angle of  $38.6^\circ$  against the vertical looking towards east, the descending pass at an angle of  $38.6^\circ$  against the vertical looking towards west. The LOS displacement rates shown in Figure 4 are relative to an arbitrarily chosen reference area located in western Sydney. Mean standard deviations ( $2\sigma$ ) of linear velocities are 1.0 mm/yr and 0.7 mm/yr for the ascending and descending data set, respectively.

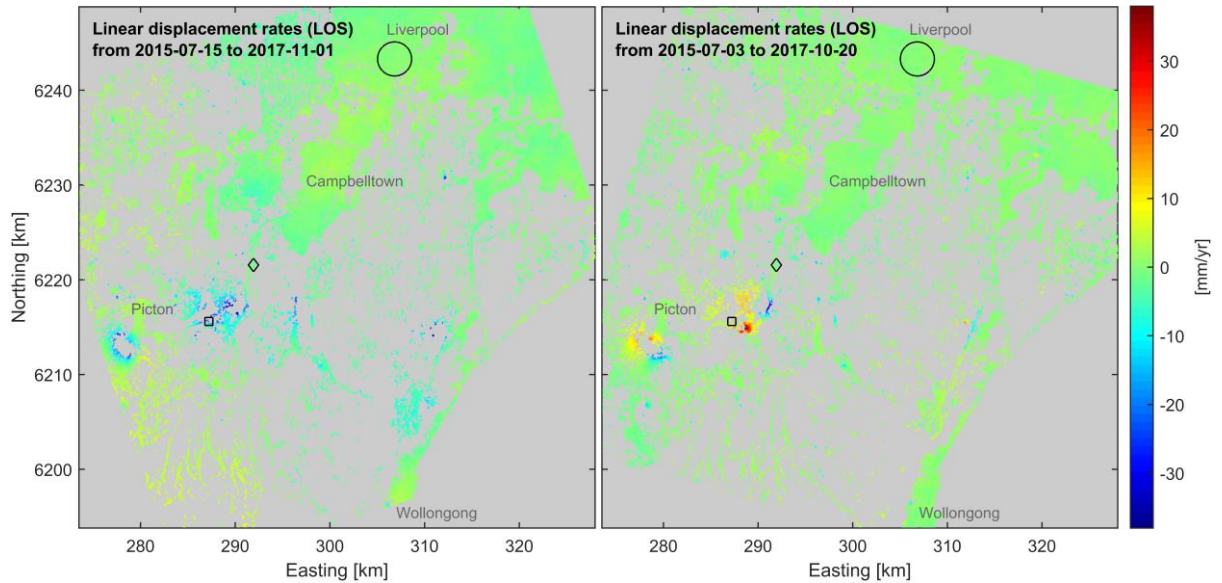


**Figure 4.** LOS displacement rates from analysis of ascending (left image) and descending (right image) Radarsat-2 data; the black circle marks the reference area located in western Sydney, the black square and diamond mark the location of site CA19 and MENA, respectively

In order to derive horizontal and vertical displacement components from InSAR, the displacement data observed in ascending and descending image geometries is mathematically combined. This is possible if LOS displacements are available (i) at the same location for all analysed tracks and (ii) within the same time period. To fulfil (i) spatial interpolation is needed as the location of PS pixels is different for each analysed stack of images. The Kriging technique (e.g. Li and Heap, 2008) is applied to interpolate LOS displacements to a 50 m grid taking into account the geostatistical properties of the displacements at each measurement epoch. The LOS displacement rates shown in Figure 4 are interpolated to a 50 m grid, where interpolation is only performed if a certain number of PS pixels is available in the surroundings of a given interpolation location. Note that the same reference area was used for InSAR analyses in both tracks in order to enable a consistent combination of ascending and descending displacement data. The time period of the available Radarsat-2 data is roughly the same for both tracks. By combining displacement rates (i.e. velocities) resulting from linear regression of the displacement time series at each grid pixel, no temporal reference is needed. Combination of epoch displacements instead of linear rates would require interpolation in time in addition to the spatial interpolation. For more information on spatial interpolation of InSAR displacements at PS pixels and data combination see Fuhrmann et al. (2015a) and Fuhrmann (2016).

From the resulting velocity fields shown in Figure 5 (East-West and Up-Down components), one can state that the northern part of the analysed area was stable in the period between July 2015 and October 2017 within  $\pm 2$  mm/yr and that several significant movements with velocities of up to 30 mm/yr occurred in the area south-west of Sydney. The combined results shown in Figure 5 demonstrate how PS-InSAR can deliver a spatial view of surface displacements, particularly when applied in urban areas, such as Sydney, where PS pixel density is high.

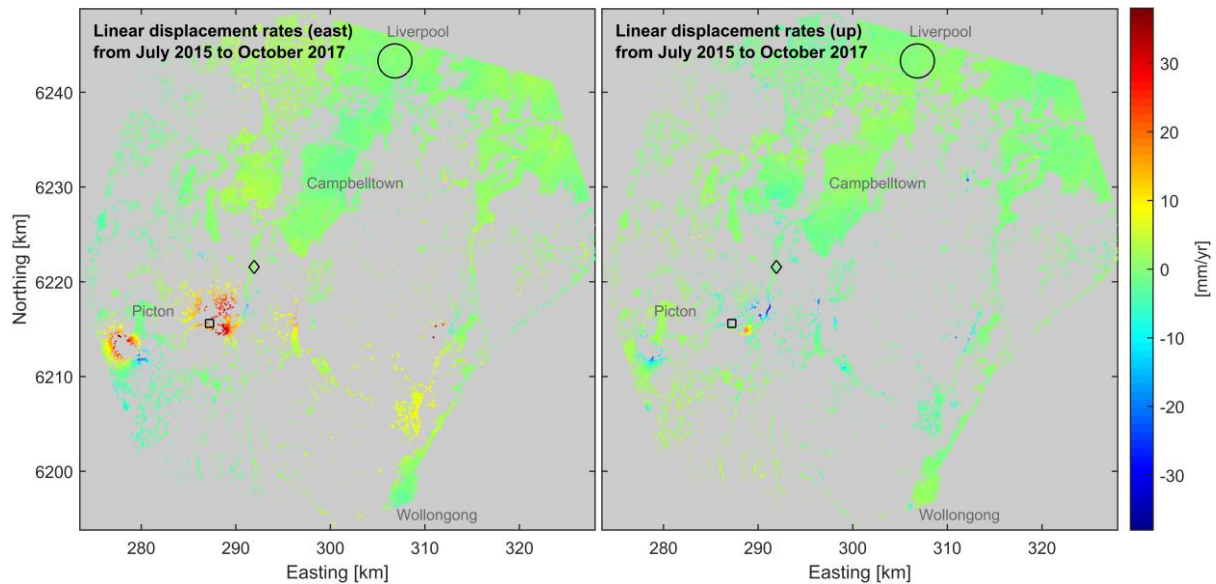


**Figure 5.** Displacement rates from combination of ascending and descending Radarsat-2 tracks, left: East component, right: Up component; the black circle marks the reference area, the black square and diamond mark the location of site CA19 and MENA, respectively

The geodetic monitoring sites enable the comparison of the displacements derived from GNSS and InSAR at the same measurement location. Figure 6 shows the LOS displacements at site CA19 (pictured in Figure 1) resulting from analysis of Radarsat-2 data since July 2016.



By that time, the CRs had been installed and show reasonable backscattering in the ascending and descending radar acquisitions. For validation, the 3D coordinate changes resulting from GPS analysis are projected into the ascending and descending LOS of the corresponding Radarsat-2 track. For the descending geometry there is a good fit between the InSAR and GPS displacements. Note that the GPS displacements are noisier compared to InSAR because of the strong influence of the GPS-derived Up component on the projected LOS displacement vector. For the ascending LOS the fit between GPS and InSAR is good for the first 10 months of the time series, but slightly worse after April 2017. This discrepancy is possibly due to unmodelled phase contributions present in the ascending pass InSAR data and could improve with the acquisition of more InSAR data.

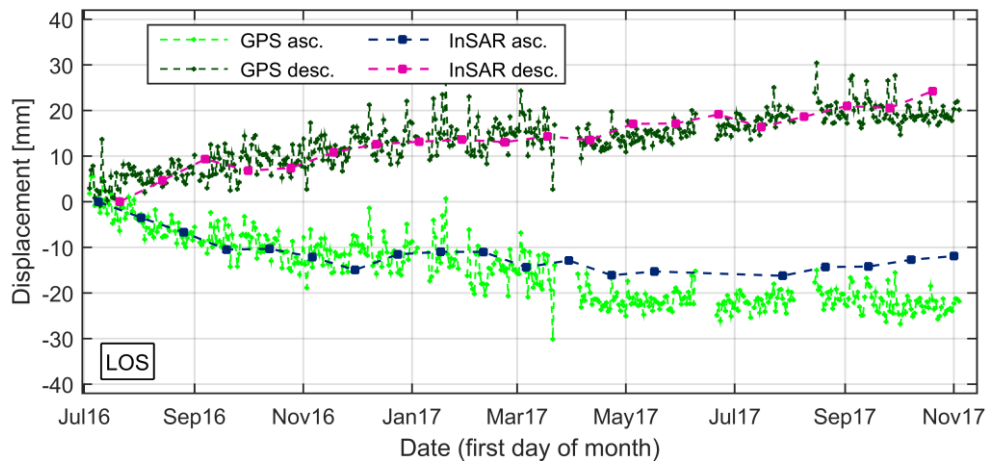


**Figure 6.** LOS displacements measured at CA19 by InSAR at ascending (asc.) and descending (desc.) CRs and by GPS at the antenna on top of the pole (see Figure 1); GPS East, North and Up components are projected into ascending and descending LOS geometry

Similar results for the agreement between GNSS and InSAR are observed at the other geodetic monitoring sites in the network. A statistical assessment of LOS displacements derived by InSAR and GNSS at the 21 GNSS sites equipped with CRs results in an average difference of 4.8 mm and 4.2 mm for the ascending and descending LOS, respectively, with most differences being within 10 mm (maximum difference of 20 mm). Consequently, one can state that relative displacements measured by both techniques agree at the level of 5 to 10 mm at our geodetic monitoring sites, but CA19 is the only site in the analysed geodetic network affected by surface displacement greater than 10 mm in magnitude.

### 3.3 GNSS multipath caused by co-located corner reflectors

Multipath effects, caused by reflections in the near-field and far-field of a GNSS antenna, distort the original GNSS signal through interference. As a consequence, all objects surrounding a GNSS antenna can potentially be sources of multipath. Hence, the metal CRs attached to the GNSS monument are likely to induce some kind of multipath to observed GNSS signals. At site MENA (Menangle, NSW, see Figure 7), GNSS data had been acquired for over three years prior to the attachment of the CRs on May 2016. This site is therefore suitable to assess the effect of potential GNSS signal interference with the CRs. Coordinate variability and standard deviations resulting from daily GPS processing are compared before and after CRs were attached at the site. A similar investigation has been performed by Parker et al. (2017) for CRs which are located several tens of meters away from a continuous GNSS

site. For this scenario, no detectable increase in the average RMS of GNSS carrier-phase residuals was found, when comparing the residuals before and after CRs were deployed. At MENA and the other geodetic monitoring sites in the area, the CRs are mounted directly underneath the GNSS antenna and may hence affect GNSS observations more significantly.



**Figure 7.** CORSnet-NSW site MENA (Menangle) before (left image) and after (right image) radar CRs have been attached to the antenna pole in May 2016.

Figure 8 displays the time series of coordinate changes since January 2013 for the East component of displacement. In order to assess the effect of the CRs on the coordinate estimates, the mean absolute difference with respect to a moving average (red line in Figure 8) is calculated for each analysed day. This measure of coordinate variability is subsequently compared for the periods before and after the CRs were attached (2013-01-19 to 2016-05-24, and 2016-05-26 to 2017-11-04, respectively). The coordinate variability and a comparison of mean standard deviations for the periods before and after CR deployment are given in Table 2. In general, a slight increase of standard deviation and coordinate variability is observed after the CR deployment for all coordinate components (East, North and Up). However, the effect is less than 0.1 mm for all components and, therefore, negligible for long-term monitoring of surface displacements. The difference in standard deviations between winter and summer months is much larger than the differences for the period before and after deployment (as seen from Figure 9). More in-depth investigations in to multipath effects induced by the CRs could include using multipath stacking maps generated for a certain analysis period (e.g. Fuhrmann et al., 2015b).

Period	Number of analysed days	Coordinate variability [mm]			2 $\sigma$ coordinate standard deviation [mm]		
		East	North	Up	East	North	Up
before	1222	0.70	0.63	3.20	1.04	1.09	3.15
after	527	0.77	0.68	3.32	1.06	1.10	3.21

**Table 2.** Statistical assessment of GNSS coordinate variability at site MENA for the period before (2013-01-19 to 2016-05-24) and after (2016-05-26 to 2017-11-04) CRs were deployed

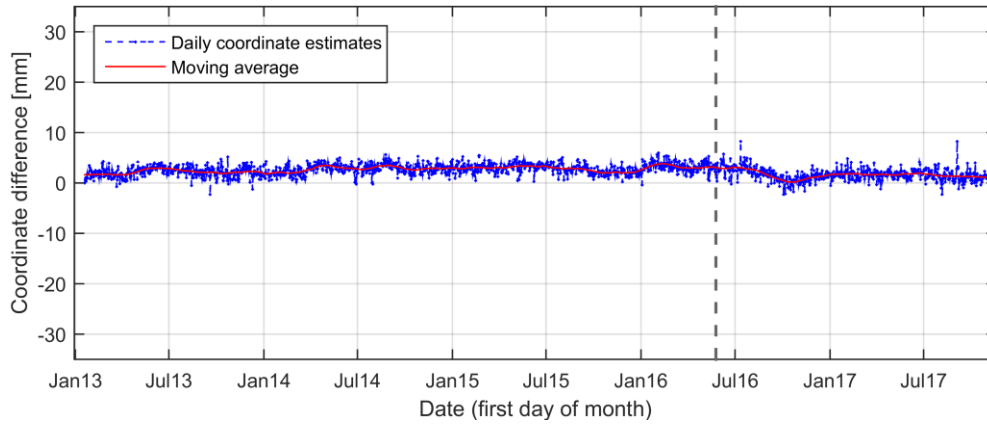


**Figure 8.** Coordinate differences (East component) at site MENA with respect to the first observed day (18 January 2013); the dashed grey line marks the date of the CR deployment on 25 May 2016

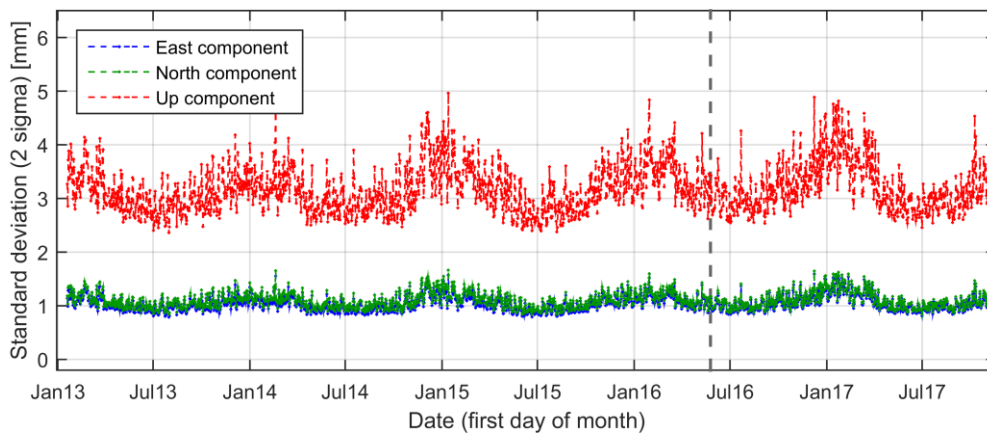


**Figure 9.** Standard deviation ( $2\sigma$ ) of daily coordinate estimates (East, North and Up component) at site MENA; the dashed grey line marks the date of the CR deployment on 25 May 2016

## 4. CONCLUSIONS

In this contribution the ability of InSAR to accurately measure surface displacements and displacement rates at a dense set of measurement points was demonstrated. The ability of satellite radar data to cover large areas presents a promising opportunity to include surface displacements detected by InSAR into national datums, particularly to update the vertical datum. In contrast to large-scale GNSS networks providing an accurate solution for continental plate tectonics, InSAR is well-suited to detect regional scale deformation phenomena. Future Australian datums could make use of InSAR as a technique to densify existing GNSS networks in order to detect and characterise ground surface deformation at various spatial scales. Furthermore, InSAR can be used to frequently update coordinates of geodetic benchmarks affected by surface deformation without the need to directly take measurements on the ground at those benchmarks.

CRs can be deployed as part of geodetic monitoring networks in order to validate displacements measured by InSAR with displacements measured at the same location by GNSS or levelling. First results of the validation of InSAR and GPS observations from co-located geodetic monitoring sites reveal good agreement at the level of 5 to 10 mm. Co-located CR/GNSS sites may serve as a local tie to incorporate InSAR into Australian datums

in the future. Validation and combination of InSAR with ground-based measurement techniques (such as GNSS or levelling) is important to account for the limitations of InSAR, which can include un-modelled atmospheric effects and the low sensitivity to North-South displacements. Statistical analysis of coordinate time series presented here has proven that potential GNSS multipath effects induced by CRs attached directly to GNSS monumentation have a negligible influence on daily site coordinates derived from GPS observations (below 0.1 mm).

The Sentinel-1 satellite mission launched in 2014 by European Space Agency (ESA) provides coverage of radar images over the entire Australian continent since October 2016 with a generally short revisit time (usually 12 days). This creates the opportunity to use InSAR on a national scale in the future. In compliance with ESA's new data policy (Aschbacher and Milagro-Pérez, 2012), Sentinel-1 data is provided by ESA completely free of charge. Therefore, it is possible to provide regular updates of InSAR deformation map products at a low cost once the data processing of the huge archive of Sentinel-1 data over Australia is streamlined and automated as far as practicable. The national GNSS network will help to link deformation maps derived at adjacent Sentinel-1 tracks and provide the opportunity to incorporate InSAR into the determination of a national vertical datum. InSAR analysis on a national scale in Australia will result in detailed and timely information on surface deformation to be used along with GNSS to update benchmark coordinates and to detect potential natural or anthropogenic deformation phenomena.

## ACKNOWLEDGEMENTS

The authors would like to thank the Geological Survey of NSW, Department of Planning & Environment, for project funding and collaboration. We are grateful to all the property owners who provided access for the installation and usage of geodetic monitoring sites on their properties. We also want to thank all colleagues at Geoscience Australia involved in the construction of geodetic monitoring sites, GNSS survey campaigns, and analysis of GNSS and InSAR data. Many thanks to Ryan Ruddick and Adrienne Moseley for internal review of the paper. This paper is published with the permission of the CEO, Geoscience Australia and the Executive Director, Geological Survey of NSW.

## REFERENCES

- Adam N, Kampes BM, Eineder M, Worawattanamateekul J, Kircher M (2003) The Development of a Scientific Permanent Scatterer System, in: Schroeder M, Jacobsen K, Heipke C, editors, *Proceedings of the Joint ISPRS/EARSeL Workshop "High Resolution Mapping from Space 2003"*, Hannover, Germany, 6–8 Oct 2003, pages 1–6
- Altamimi Z, Rebischung, P, Métivier, L, and Collilieux, X (2016) ITRF2014: A new release of the International Terrestrial Reference Frame modeling nonlinear station motions, *Journal of Geophysical Research: Solid Earth*, 121(8): 6109–6131
- Aschbacher, J. and Milagro-Pérez, M. P. (2012) The European Earth monitoring (GMES) programme: Status and perspectives, *Remote Sensing of Environment* 120: 3–8
- Casu F, Manzo M, Lanari R (2006) A quantitative assessment of the SBAS algorithm performance for surface deformation retrieval from DInSAR data, *Remote Sensing of Environment*, 102:195–210.



- Choi DCT, Wong JYK, Chan, BSB (2007) Investigation on GPS Heighting Accuracy with the use of Hong Kong Satellite Positioning Reference Station Network (SatRef), in: Strategic Integration of Surveying Services, FIG Working Week 2007, Hong Kong SAR, China, 13-17 May 2007.
- Dach R, Lutz S, Walser P, Fridez P (2015) Bernese GNSS Software Version 5.2 (User manual), *Bern Open Publishing*. ISBN: 978-3-906813-05-9
- Ferretti A, Prati C, Rocca F (2000) Nonlinear subsidence rate estimation using permanent scatterers in differential SAR interferometry, *IEEE Transactions on Geoscience and Remote Sensing*, 38(5):2202–2212
- Ferretti A, Prati C, Rocca F (2001) Permanent scatterers in SAR interferometry, *IEEE Transactions on Geoscience and Remote Sensing*, 39(1):8–20
- Ferretti, A, Savio G, Barzaghi R, Borghi A, Musazzi S, Novali F, Prati C and Rocca F, 2007 Submillimeter accuracy of InSAR time series: Experimental validation, *IEEE Transactions On Geoscience And Remote Sensing*, 45(5): 1142-1153
- Fuhrmann T, Caro Cuenca M, Knöpfler A, van Leijen FJ, Mayer M, Westerhaus M, Hanssen RF, Heck B (2015a) Estimation of small surface displacements in the Upper Rhine Graben area from a combined analysis of PS-InSAR, levelling and GNSS data, *Geophysical Journal International*, 203(1):614–631
- Fuhrmann T, Luo X, Knöpfler A, Mayer M (2015b) Generating statistically robust multipath stacking maps using congruent cells, *GPS Solutions*, 19(1):83–92
- Fuhrmann T (2016) Surface Displacements from Fusion of Geodetic Measurement Techniques Applied to the Upper Rhine Graben Area, Ph.D. Thesis, Karlsruhe Institute of Technology (KIT), available online: <http://dx.doi.org/10.5445/IR/1000056073>.
- Garthwaite MC (2017) On the Design of Radar Corner Reflectors for Deformation Monitoring in Multi-Frequency InSAR, *Remote Sensing* 9, 648
- Garthwaite MC, Nancarrow S, Hislop A, Thankappan, M, Dawson JH, Lawrie S (2015) Design of Radar Corner Reflectors for the Australian Geophysical Observing System, *Geoscience Australia*, Canberra, Australia.
- Hofmann-Wellenhof, B, Lichtenberger, H, and Wasle, E (2008) *GNSS – Global Navigation Satellite Systems*, Springer, Vienna, Austria.
- Hooper A, Zebker HA, Segall P, Kampes, BM (2004) A new method for measuring deformation on volcanoes and other natural terrains using InSAR persistent scatterers, *Geophysical Research Letters*, 31(23):1–5
- Hooper A, Segall P, Zebker HA (2007) Persistent scatterer interferometric synthetic aperture radar for crustal deformation analysis, with application to Volcán Alcedo, Galápagos, *Journal of Geophysical Research: Solid Earth*, 112(B7):1–21
- ICSM (2017), Geocentric Datum of Australia 2020 Technical Manual Version 1.0, *Intergovernmental Committee on Surveying and Mapping, Australia*.
- Kampes BM (2005) Displacement parameter estimation using permanent scatterer interferometry. *Ph.D. Thesis*, Delft University of Technology, Delft, The Netherlands.
- Li J, Heap, AD (2008) A Review of Spatial Interpolation Methods for Environmental Scientists. Record 2008/23. Geoscience Australia, Canberra, Australia.
- Parker AL, Featherstone WE, Penna NT, Filmer MS, Garthwaite MC (2017) Practical Considerations before Installing Ground-Based Geodetic Infrastructure for Integrated InSAR and cGNSS Monitoring of Vertical Land Motion, *Sensors*, 17(8)
- Torge, W and Müller, J (2012) *Geodesy* (fourth edition), de Gruyter, Berlin, Germany.
- Warrington RB (2017) National Measurement (Recognized-Value Standard of Measurement of Position) Determination 2017, *Federal Register of Legislation, Australian Government*.